NASA Technical Memorandum 4768

Titanium Honeycomb Panel Testing

W. Lance Richards and Randolph C. Thompson

October 1996

NASA Technical Memorandum 4768

Titanium Honeycomb Panel Testing

W. Lance Richards
Dryden Flight Research Center
Edwards, California

Randolph C. Thompson
PRC Inc.
Edwards, California

National Aeronautics and
Space Administration

Office of Management

Scientific and Technical
Information Program

1996

TITANIUM HONEYCOMB PANEL TESTING

W. Lance Richards

NASA Dryden Flight Research Facility
Edwards, California

Randolph C. Thompson

PRC Inc.
Edwards, California

ABSTRACT

Thermal–mechanical tests were performed on a titanium honeycomb sandwich panel to experimentally validate the hypersonic wing panel concept and compare test data with analysis. Details of the test article, test fixture development, instrumentation, and test results are presented. After extensive testing to 900 °F, nondestructive evaluation of the panel has not detected any significant structural degradation caused by the applied thermal–mechanical loads.

NOMENCLATURE

Al	aluminum
DACS	Data Acquisition and Control System
LID	liquid interface diffusion
Mo	molybdenum
NDI	nondestructive inspection
Si	silicon
Sn	tin
Ti	titanium
TiHC	titanium honeycomb core
V	vanadium
Zr	zirconium
ΔT	temperature change from initial reference temperature, °F

INTRODUCTION

Honeycomb-core sandwich panels were identified in the late 1960's as one of several candidate concepts for use on high-speed aircraft [1]. In early investigations, honeycomb panels exhibited problems with the bonding between the facesheets and the honeycomb core. Improved bonding techniques, such as the liquid interface diffusion (LID) process (LID bonding is a Rohr Proprietary process), have resulted in the reemergence of titanium honeycomb panels as leading candidates for the wing panels of a Mach 5 aircraft.

Personnel at the National Aeronautics and Space Administration (NASA) Dryden Flight Research Facility (DFRF) have recently completed thermal–mechanical tests on two LID-bonded titanium honeycomb panels. The test program was based on a study conducted at the NASA Langley Research Center (LaRC) in which two titanium wing structure concepts were analyzed for use on a Mach 5 vehicle [2]. This study led to the development and fabrication of two LID-bonded titanium honeycomb wing panels designed to survive the thermal stresses produced in a 900 °F thermal environment. A test program was developed at NASA DFRF to demonstrate the wing panel design and fabrication, evaluate the LID bonds between the core and facesheets, and correlate test data with a finite-element analysis performed at NASA LaRC. The test and modeling techniques were refined before exposing the panel to the ultimate 900 °F thermal environment. This ensured that the thermal stresses produced in the panels were representative of Mach 5 flight conditions and that preliminary test data and analysis were compatible. This paper describes some of the difficulties overcome in the testing and analysis to successfully demonstrate these wing panels for use on a Mach 5 vehicle. Details of the panel evaluation tests including the test article, instrumentation, test setup development, and results are discussed.

TEST OBJECTIVES AND METHODOLOGY

The titanium honeycomb-core (TiHC) wing panels were required to survive the thermal stresses produced in Mach 5 flight. Figure 1 depicts such a wing panel as part of a multipanel array in the outboard wing section of the airplane. During the aerodynamic heating encountered in a typical mission, each panel will be prevented from rotating about its edges by the surrounding wing structure. To simulate these flight conditions in the laboratory, the preferred testing approach is to mount the test article with additional buffer panels on a fixture representing the wing structure. The test article, placed in the center of the multipanel array, is less sensitive to unrealistic boundary effects in this arrangement. When simulated flight temperatures are applied to the entire

structure, realistic thermal stresses develop naturally in the center panel. Although this approach is highly desirable and has produced successful results [3], it is also very expensive.

An alternative test approach was pursued in this program. Because of budget constraints, two TiHC wing panels were tested separately and not in a multipanel array. The same ideal thermal-structural loads determined in Ref. [2] were applied in a single panel test setup. The original test goals were to apply uniform temperatures across the upper wing panel skin, prevent all four panel edges from rotating, and allow the panel to thermally expand in-plane. It was recognized from the outset that producing the proper boundary conditions on a single panel would be very difficult, if not impossible to achieve.

The test program was divided into mid- and high-temperature thermal–mechanical tests. The first phase was to thermally cycle the wing panels 50 times from room temperature to 600 °F. The second phase was to thermally cycle the wing panels 50 times from room temperature to 900 °F. Exposing the panels to the 100 transient thermal-stress cycles also was done to assess low cycle fatigue performance. Nondestructive inspection (NDI) was performed after manufacturing and after each of the 50 thermal cycles to verify the core to facesheet bonding integrity.

TEST DESCRIPTION

Test Article

Figure 2 shows one of two TiHC sandwich panels built under a contract to Lockheed Aeronautical Systems Co. (Calabasas, California) and Rohr Industries, Inc. (Chula Vista, California). The panels measure 23 in. square and consist of two 0.060-in.-thick titanium alloy (Ti-6Al-2Sn-4Zr-2Mo-.09Si) (Ti-6242-Si) facesheets LID-bonded to a 0.69-in.-thick honeycomb core. The core is formed into 0.1875-in. hexagonal cells from 0.002-in.-thick titanium alloy (Ti-6Al-4V) foil. Edge closeouts are brazed to the core on all four edges and are made from 0.020-in.-thick Ti-6242-Si. Ti-6Al-4V bearing plates measuring 1.5 in. square and 0.125 in. thick were fastened to the perimeter of the upper and lower panel surfaces.

Instrumentation

The panels were instrumented with sensors capable of measuring surface strains, temperatures, and out-of-plane deflections at 600 and 900 °F. The instrumentation included conventional foil strain gages arranged in a rectangular rosette for use at 600 °F. Foil strain gages and weldable strain gages were used at 900 °F. Duplex glass braid insulated type K thermocouples were used at 600 and 900 °F. Deflection potentiometers also were used throughout the test program to measure out-of-plane panel deformations. The sensors were installed on one quadrant of the upper and lower facesheets to utilize the two planes of symmetry that exist about the panel centerline axes. Figure 3 shows the upper surface of a panel instrumented for testing at 900 °F.

Data Acquisition and Thermal Control

Data acquisition and adaptive digital thermal control were accomplished by using the Data Acquisition and Control System (DACS) Thermostructures Research Facility at the NASA DFRF [4]. The DACS was used to apply the same 600 and 900 °F temperature profiles to the upper surface of the panel as determined in a heat transfer analysis [2]. A thermocouple located at the center of the upper surface was used in the DACS feedback algorithm to impose a predicted flight temperature profile by varying the power supplied to the heaters. For preliminary testing, thermocouples located on the side closeouts were used to control the edge temperatures.

The DACS maximum allowable system measurement error is ± 0.15 percent of reading or ± 20 μV, whichever is greater. Therefore, for a ± 20 μV strain measurement input from a single active arm strain gage with a 4-V direct current (DC) excitation voltage, the error band is ± 8 μin/in. However, this error is reduced with additional active arms and higher excitation voltages. Similarly, a type K thermocouple measurement error with a ± 20 μV input is equivalent to ± 0.9 °F.

TEST DEVELOPMENT

This section describes the process used to develop a test to adequately achieve the program objectives.

Initial Test Setup Description

Figure 4(a) depicts the in-flight configuration of a titanium wing panel mounted on a wing structure. Figure 4(b) shows the single-panel concept used in this test. The top and center schematics show that when one surface of a simply-supported wing panel is heated, the panel will bend out-of-plane to alleviate thermal stresses. The bottom schematic shows the boundary conditions desired in the test. The goal was to prevent rotation at the panel edges while allowing in-plane translation. The upper and lower bolts shown in Fig. 5 were offset to react against panel rotation as the upper surface of the panel was heated. The 0.75-in. perpendicular distance between the bolts was designed to maximize the moment restraint and minimize thermal shading at the panel edges from the overhead heat source. Fifty-two separate restraint mechanisms were located around the perimeter of the panel (13 on each side). The restraint mechanisms consisted of a 0.5-in. by 0.75-in. by 1.375-in. stainless steel load pad and UNF 3/8-24 high-strength steel bolts. The end of each bolt had a spherical radius that fit into a spherical socket in the load pad. The load pads, bearing plates, and bolts are shown in Fig. 5. The bolts in turn were supported by large structural steel members consisting of angle beams (L6 X 6 X 0.75), two 0.75-in.-thick back plates and two to three C beam stiffeners. Angle beam stiffeners were welded to the

angle between every third or fourth bolt. High-temperature lubricant, located between the load pads and bearing plates, allowed the panel to thermally expand in-plane. Small gold-plated reflectors were used to heat the sides of the panel and help offset the conduction losses at the panel edges caused by the massive test fixture.

The upper facesheet surface was heated by infrared quartz lamp heaters located 6 in. above the test article. Figure 6 shows the array of heating units used. Eight gold-plated reflectors, each containing 6 12-in.-long lamps, were capable of producing 48 kW of total power.

Comparison of Preliminary Test Data With Finite-Element Analysis

Both panels were exposed to 50 transient heating cycles from room temperature to 600 °F in the initial test setup. Temperature at the center of the upper surface was controlled to within ±5 °F of the 600 °F transient heating profile calculated in Ref. [2]. The side heaters were also used to heat the panel edges in an attempt to reduce heat loss at the boundaries. The edge restraint mechanisms were brought into contact with the panel edges to react against the panel edge rotation as the panel thermally distorted during the heating profile.

After the initial testing, the preliminary data were compared with a finite-element analysis performed at NASA LaRC. Preliminary data–analysis correlation showed that the analytical strains were significantly higher than the measured strains. The analysis also predicted that the magnitudes of the compressive upper surface strains were equal to the lower surface tensile strains. However, the measured upper surface strains were almost twice the magnitude of the lower surface strains. The measured and calculated deflections at the panel center disagreed by 16 percent [5].

Evaluation of Preliminary Test Techniques

The following testing issues required further investigation to understand why experimental and analytical results did not compare well.

Strain Measurements. One of the largest uncertainties in the strain gage measurement during the 600 °F testing was the apparent strain in the gage installation. Apparent strain is defined as the strain produced by the difference in thermal expansion between the gage and the material to which it is attached. A smaller component of apparent strain is caused by the change in gage factor and the temperature coefficient of resistivity of the gage material with temperature. Normally, apparent strain is characterized by installing strain gages on coupons in which both the gage and the coupon are assumed to represent those used in the test. After the instrumented coupon is heated several times to the expected temperature range, the apparent strain correction curve is obtained by averaging the thermal cycle data sets. Figure 7 shows apparent strain as a function of temperature for a bonded foil strain gage on Ti-6242-Si. This curve is then used after testing to correct the test data for apparent strain at any given test temperature.

Apparent strain tests were originally performed on coupons made from the same material as the panel facesheets. To verify that the strain gages were well-characterized for apparent strain, additional apparent strain tests were conducted using the instrumented test article instead of coupons. The advantage in this method was that the actual strain gages and the test article could be uniquely characterized for apparent strain. This approach avoids assumptions about how well the coupon tests represent the gages and test article used in the heating tests. The apparent strain correction technique assumes, however, that the stress-induced strain in the built-up panel is negligible and that only the apparent strain is measured. The maximum difference between the panel and coupon apparent strain curves was approximately 90 μin/in. The data precision was also improved from ±50 to ±25 μin/in. by repeating the apparent strain tests.

Boundary Conditions. Another uncertainty in the test was the degree of end fixity the test fixture provided in the prevention of the panel edge rotation. Although the test fixture was to simulate a perfectly fixed end condition, achieving perfect end fixity in the laboratory is almost impossible [6]. This is especially true when thermal loads are applied because of the thermoelastic nature of materials. The true edge restraint provided by the test fixture was necessary to produce an accurate finite-element model of the panel.

Several tests were conducted to resolve the unknown test fixture stiffness. Figure 8 shows the test setup to quantify the degree of end fixity provided by the test fixture. An aluminum beam was installed in the test fixture and subjected to a mechanical load by the hydraulic jack shown at the bottom of the figure. The beam deflection was measured by dial gauges shown above the beam. The load cell shown at the bottom of the figure was used to measure the mechanical load applied to the beam. The same moment expected in the heated panel was used to determine the equivalent mechanical load to be applied to the aluminum beam. Comparisons of the measured deflections with simple beam theory showed the fixture provided approximately 35 percent of a fixed beam. These tests explained why the measured strains in the wing panel tests were much lower than those predicted from an analysis which assumed perfect end fixity.

Temperature Distributions. Additional heating tests were required to isolate how the top and side heaters individually affected the strain gage measurements. In these tests, the top heating profile was applied to the panel without heating the panel edges. Likewise, the side heating profile was applied to the panel edges without heating the upper panel surface.

The top heating test revealed that in-plane thermal gradients caused by the shaded panel edges produced

compressive stresses to the panel. These compressive stresses added to the upper surface compressive stresses and subtracted from the lower surface tensile stresses. This explained why the magnitude of the upper surface strains was larger than the magnitude of the lower surface strains. Test results also showed that although the side heaters produced more uniform temperatures on the upper panel surface they also reduced the magnitude of the stresses in the upper facesheet.

Evaluation–Modification of Preliminary Modeling Techniques

The test setup design process also uncovered analytical issues that led to the refinement of the finite-element model. These refinements, originally described in Ref. [5], included the following improvements. (1) The model was refined by utilizing the two planes of symmetry in the panel. Although the model was reduced from a full-panel model to a one-quarter-panel model, the number of degrees of freedom in the analysis were increased tenfold. (2) The axial rod and shear web elements used in the original model were replaced with plate and solid elements. The plate elements were used to represent the panel facesheets and the solid elements represented the honeycomb core. These elements enabled the use of anisotropic stiffness coefficients to better model the behavior of the honeycomb core. (3) Another significant improvement to the test data and analysis correlation was gained when the actual test temperatures were used in the model instead of the constant temperature distribution assumed in the original model. Therefore the refined analysis was able to more appropriately simulate the stresses produced by the large in-plane temperature gradients measured in the test. (4) The new finite-element model also included temperature-dependent physical properties which were not used in the initial model.

Final Comparison of Preliminary Test Data With Refined Finite-Element Analysis

Although the panel stresses were far lower than the stress levels predicted in Ref. [2], major improvements were made that resulted in better correlation between the experimental data and the analysis. This was essential before conducting the 900 °F evaluation tests. The measured upper surface strains were in good agreement with the calculated values. The maximum difference between measured and calculated lower surface strains was 65 μin/in. The measured and calculated center panel deflections differed by less than 5 percent.

Final Test Setup Description

The aluminum beam test results showed that the test fixture used in the original 600 °F thermal cycle tests was not of sufficient stiffness to produce the stress levels necessary to validate the wing panel concept. The test fixture was modified to improve this stiffness. Figure 9 shows the stiffened test fixture moment restraint. The most significant modification to the fixture was the removal of the side heaters because this allowed the welding of a 0.75-in.-thick steel plate close to the panel edges. Consequently, the moment arm was reduced by approximately 75 percent, greatly improving the test fixture stiffness at the panel attachment area. Figure 10 compares the initial and final test fixture configurations. Seventy-two additional angle beam stiffeners were welded to the fixture to prevent local deflections in the angle beams at the restraint mechanisms. Large structural steel I beams (W8 X 24) were welded to the back plates to further increase the test fixture stiffness.

Figure 11 presents the edge-moment calibration test results for the final test fixture. The center deflection of a simply-supported and a fixed-beam under the application of a centrally-located concentrated load were determined from simple beam theory as functions of load. The simply-supported and fixed-beam deflection curves are depicted by the uppermost and lowermost lines, respectively. The experimental data from the beam tests are shown between these two theoretical curves. This figure shows the improvement in test fixture stiffness achieved with the final test fixture. The test fixture edge fixity was improved from 35 to 75 percent of a perfectly fixed restraint.

Test Procedure Modifications

The test procedures were also modified as a result of the test technique evaluation studies. Instead of trying to impose the anticipated in-flight heating and boundary conditions to the panel, the test procedures were changed to impose the stress levels predicted in Ref. [2]. These stresses were produced in the panels by increasing the panel heating rate and applying additional bending moments at the panel edges. The combination of mechanical and thermal stress was varied until the proper stresses were produced in the panel. The restraint mechanisms, originally designed to simply react against thermal distortion, were used to mechanically induce a moment at the panel edges. The heating rate imposed in the preliminary tests was increased from 3.5 to 15 °F/sec to produce a higher thermal gradient and hence higher compressive stresses in the facesheet.

RESULTS AND DISCUSSION

The final test fixture was designed and fabricated to provide increased edge fixity. Test procedures were modified and several 600 °F checkout tests were performed before 50 of the 900 °F cycles were run.

Figure 12 shows the measured strain time history at the center of the panel on the upper and lower facesheets for a representative thermal cycle to 600 °F. Before heat was applied to the panel, a preload was applied to the bolts to induce a mechanical moment on the panel. The strain gage output resulting from this mechanically-induced load is shown at the beginning of the profile in Fig. 12. At approximately 100 sec, a 15 °F/sec temperature profile was applied to the upper surface of the panel. The heating profile

applied to the upper facesheet caused a temperature gradient (ΔT) through-the-thickness and in-the-plane of the panel. A schematic of the heating condition and the resulting temperature distribution from a representative test is shown in Fig. 13. The panel temperature sharply declines at the edges because the test fixture shades the panel border from radiant heat. The test evaluation studies showed that these in-plane thermal gradients cause significant compressive stresses which add to the upper surface compressive strains and subtract from the lower surface tensile strains. The upper surface strains shown in Fig. 12 are larger in magnitude than the lower surface strains because of the additional compressive stresses produced by the in-plane ΔT.

The measured strains were converted to stress values using a strain gage rosette reduction analysis. Table 1 compares these experimentally-determined stresses with the target stresses necessary to validate the concept. This table shows that the upper facesheet stress levels achieved in the final test setup were in 2-percent agreement with the target stress. The lower facesheet stresses do not compare as well because of the compressive stress produced by the in-plane ΔT. However, the upper surface center stresses produced in the final test fixture moment restraint were sufficient to demonstrate the panel concept.

After the 600 °F checkout tests were conducted using the final test fixture, 50 of the 900 °F thermal cycles were conducted on the same panel. The experimental data and analysis correlation from these tests is ongoing. This panel was subjected to NDI before and after the 900 °F thermal cycles. Figure 14 is a photo of an x ray of one quadrant of the panel after 50 of the 900 °F cycles. Examination of the test results has not revealed any core-to-facesheet disbonding.

CONCLUDING REMARKS

A titanium honeycomb-core sandwich panel has been thermally and mechanically tested to evaluate the panel concept and compare the results with analysis. The test techniques described were used to test the panel to 600 and 900 °F at predetermined stress levels. The panel survived more than 100 of the 600 °F thermal cycles and 50 of the 900 °F thermal cycles. Heating profiles were applied to the panel by radiant heat using quartz lamps and gold-plated reflectors. Initially, the measured strains were lower than finite-element analysis because of difficulties in both simulating and modeling complex boundary conditions. The test and modeling techniques were refined to ensure that the thermal stresses produced in the panels were representative of Mach 5 flight conditions and that preliminary test data and analysis were compatible. Stress levels required to validate the wing panel were obtained by varying the mechanically-induced bending moments at the panel edges and by varying the through-the-thickness temperature gradients. In-plane thermal gradients on the upper facesheet increased the upper facesheet compressive stresses to the stress levels necessary to achieve the test objectives.

REFERENCES

1. Plank, P.P., Sakata, I.F., Davis, G.W., and Richie, C.C., *Hypersonic Cruise Vehicle Wing Structure Evaluation*, NASA CR-1568, 1970.

2. Taylor, Allan H., Jackson, L. Robert, Cerro, Jeffrey A., and Scotti, Stephen J., "Analytical Comparison of Two Wing Structures for Mach 5 Cruise Airplanes," *J. of Aircraft*, vol. 21, no. 4, Apr. 1984, pp. 272–277.

3. Fields, Roger A., Reardon, Lawrence F., and Siegel, William H., *Loading Tests of a Wing Structure for a Hypersonic Aircraft*, NASA TP-1596, 1980.

4. Zamenzedah, Behzad, Trover, William F., and Anderson, Karl A., "DACS II - A Distributed Thermal/Mechanical Loads Data Acquisition and Control System," *Proceedings of the International Telemetering Conference, San Diego, CA, Oct. 26–29, 1987*, 1987, pp. 737–752.

5. Jones, Stuart C., and Richards, W. Lance, "Titanium Honeycomb Panel Thermostructural Test and Analysis," *Workshop on Correlation of Hot Structures Test Data With Analysis*, NASA CP-3065–Vol. II, 1990, pp. 118–175.

6. Roark, Raymond J., and Young, Warren C., *Formulas for Stress and Strain*, Fifth ed., McGraw-Hill Book Co., NY, 1975, pp. 325.

Table 1: Comparison of target and experimentally-determined stresses

	Stress, lb/in^2	
	Upper surface	Lower surface
Target	−25544	25127
Experiment–final fixture	−26100	18700

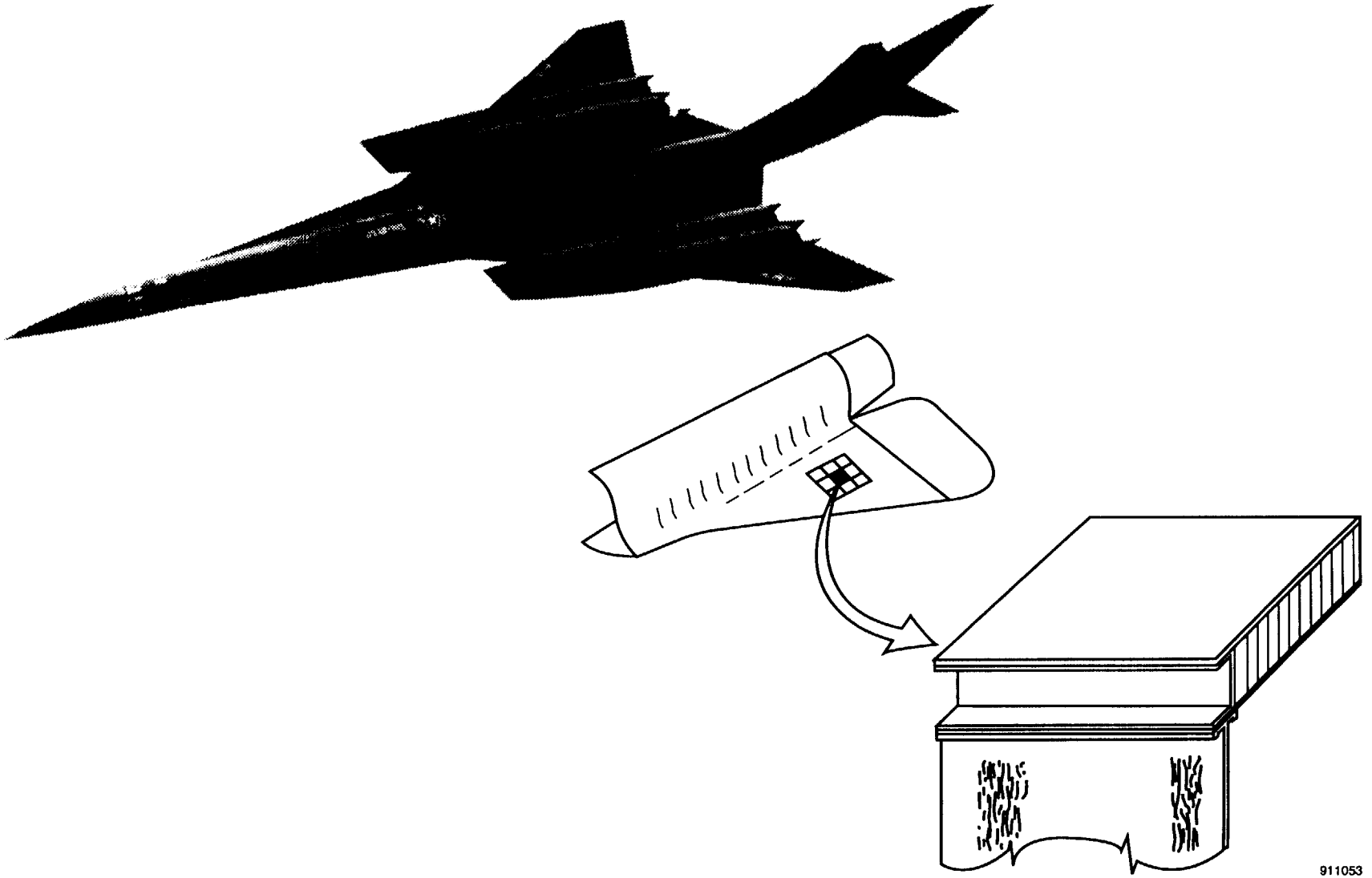

Fig. 1: Mach 5 vehicle honeycomb-core sandwich panel wing structure

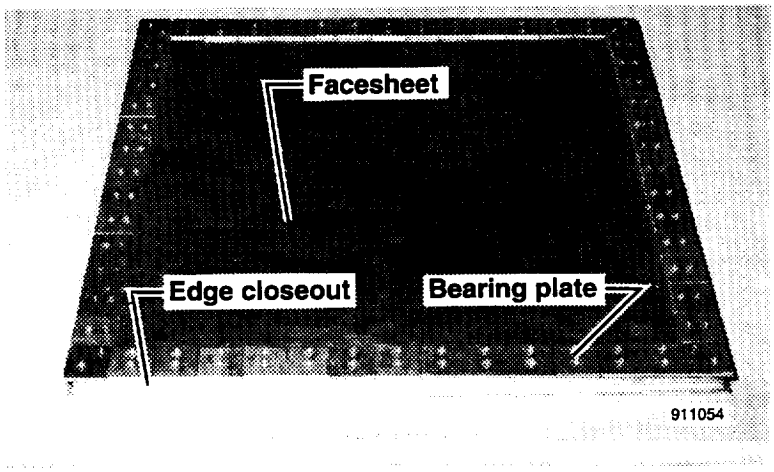

Fig. 2: TiHC sandwich panel

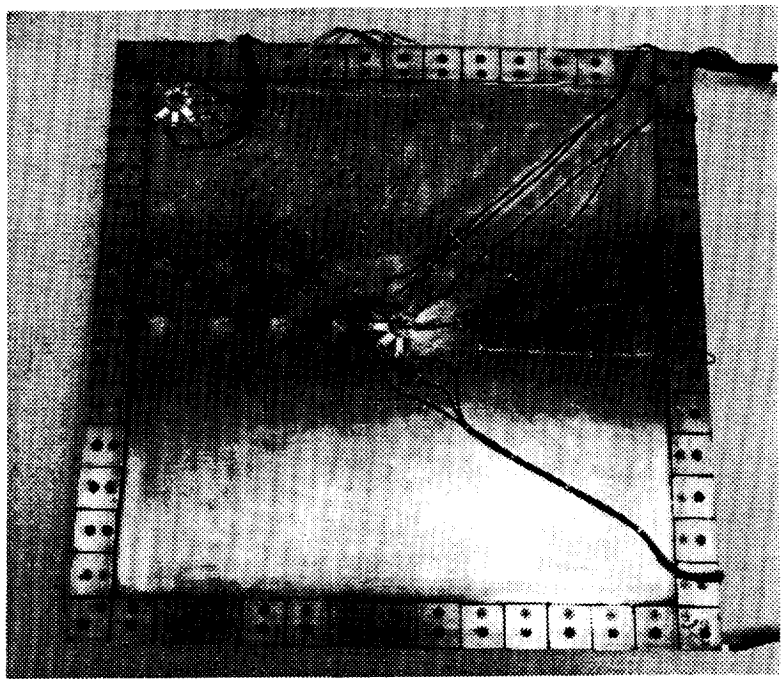

EC90 354-24

Fig. 3: TiHC sandwich panel instrumentation

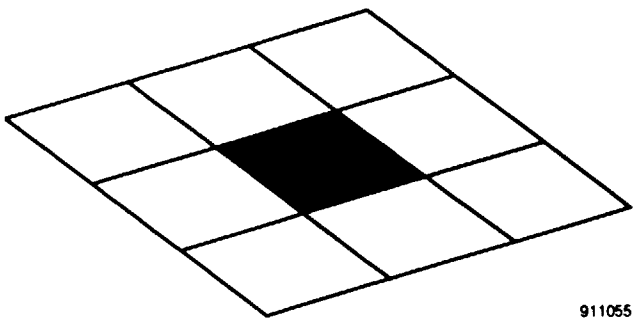

(a) Multipanel test configuration

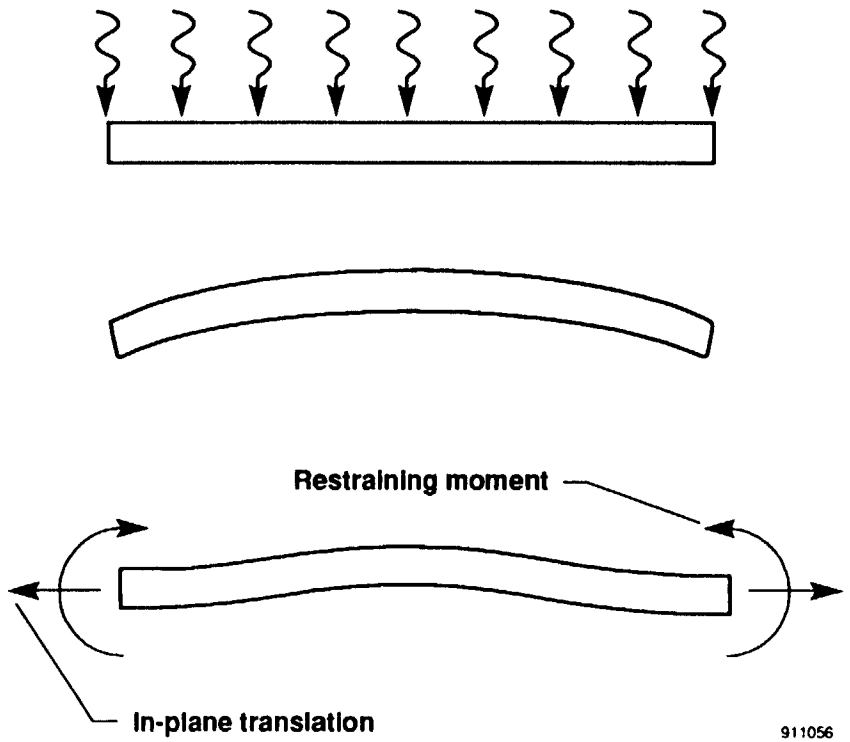

(b) Single-panel test boundary conditions

Fig. 4: Panel boundary conditions

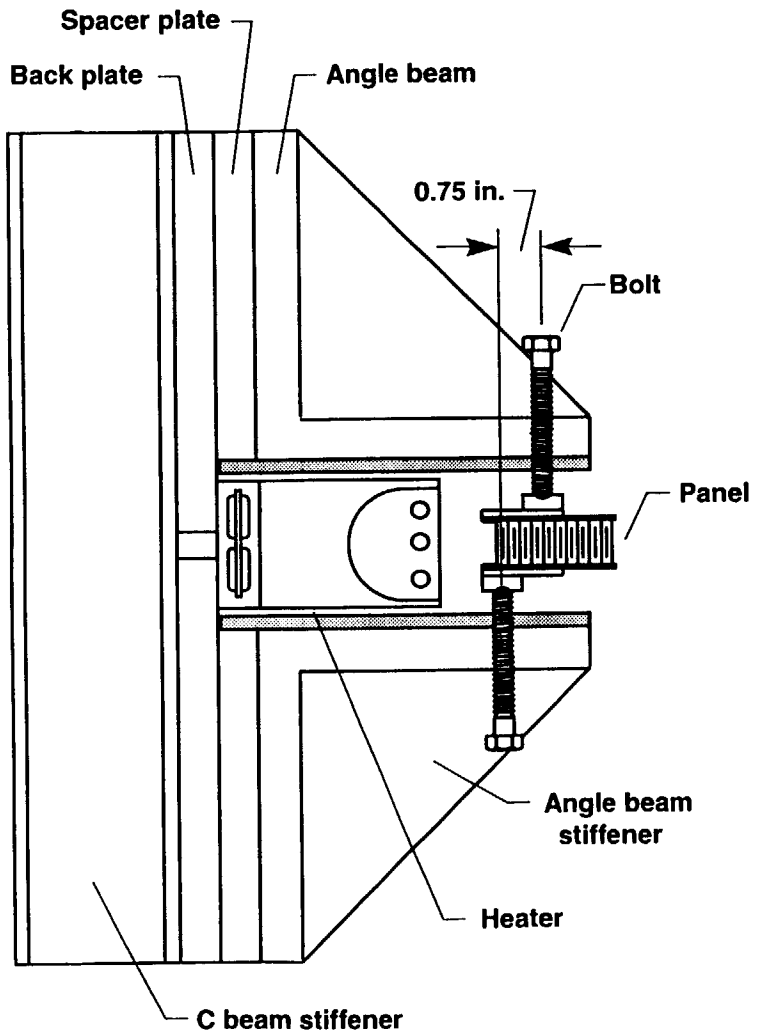

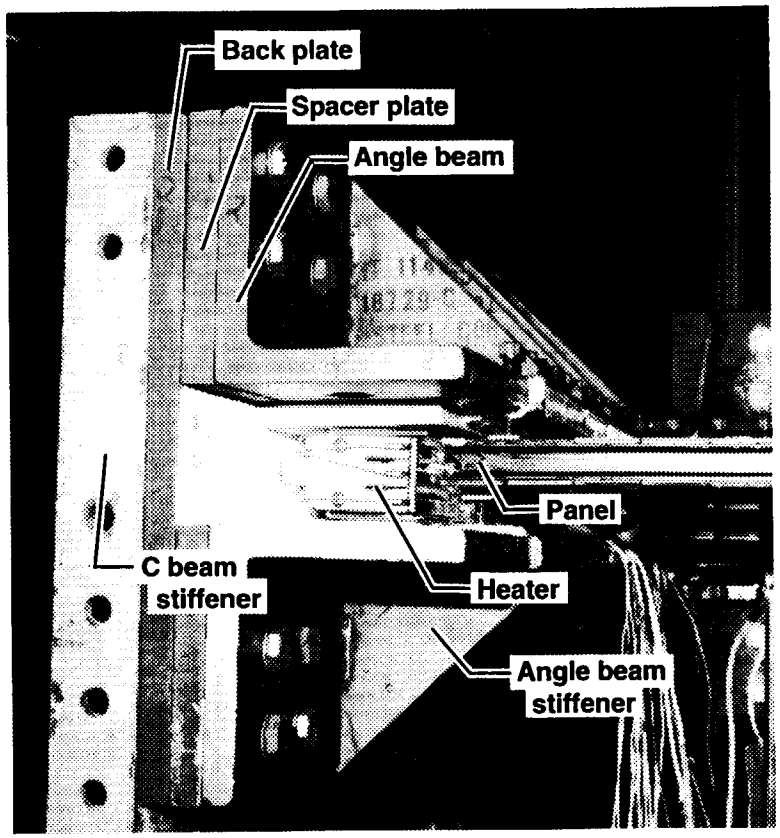

911057

Fig. 5: Initial test fixture moment restraint

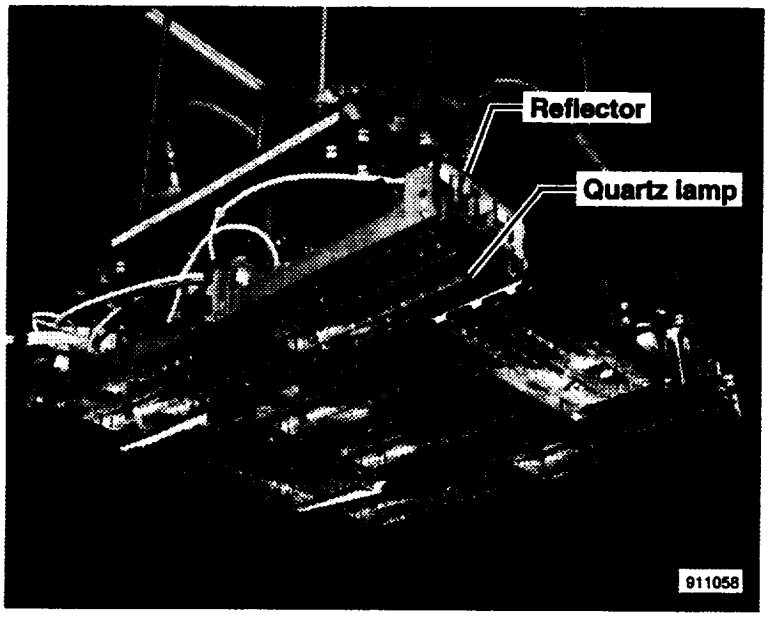

Fig. 6: Quartz lamp radiant heater

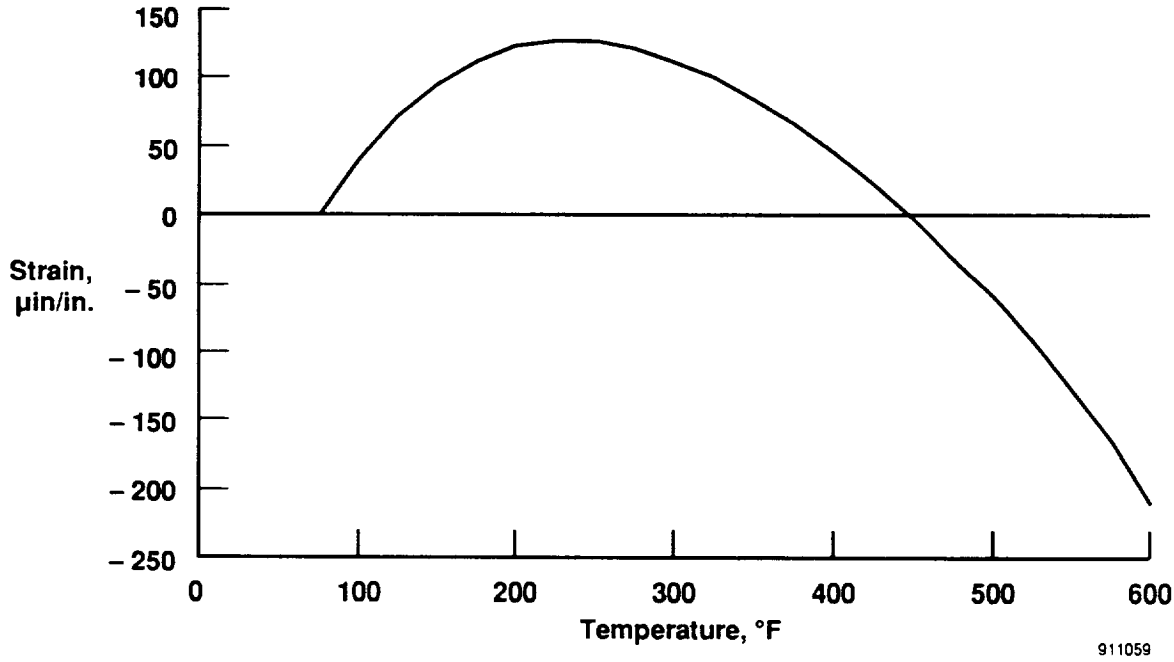

Fig. 7: Typical apparent strain curve for a bonded foil strain gage on Ti-6242-Si

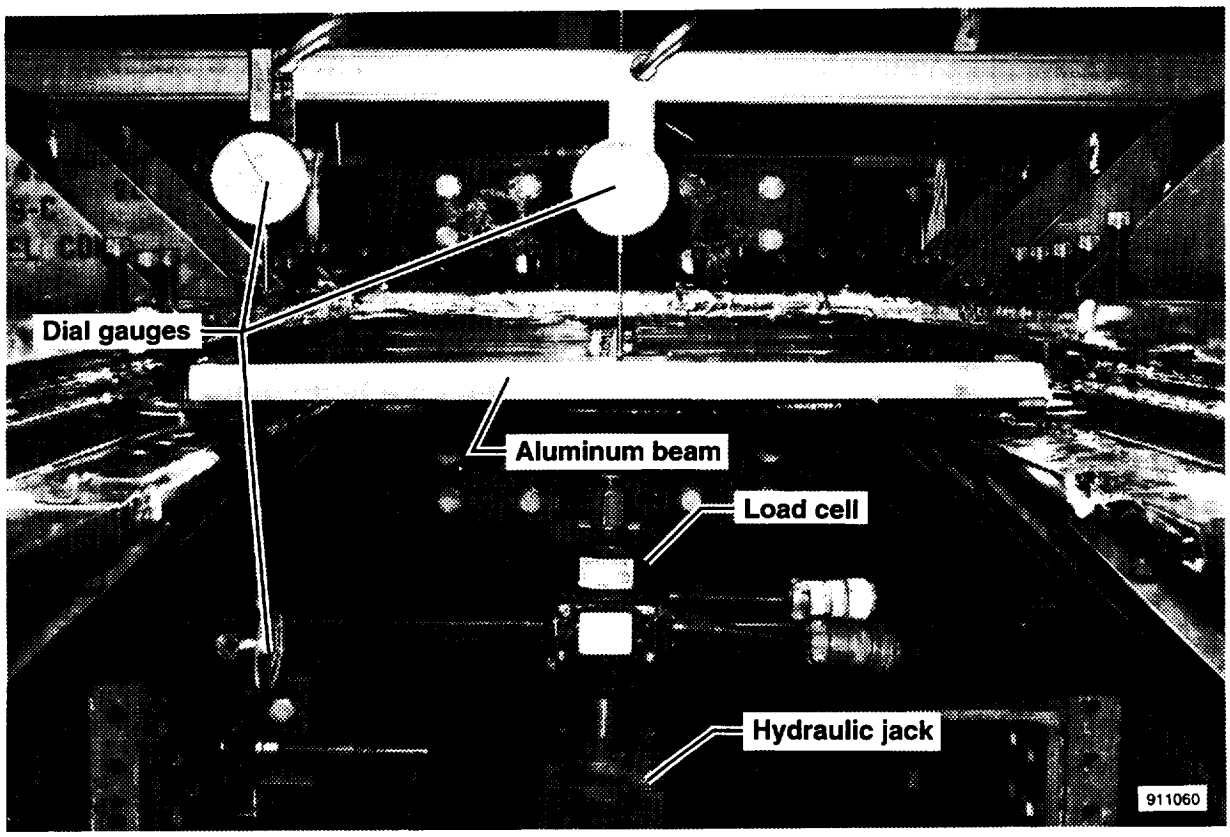

Fig. 8: Edge moment calibration test setup

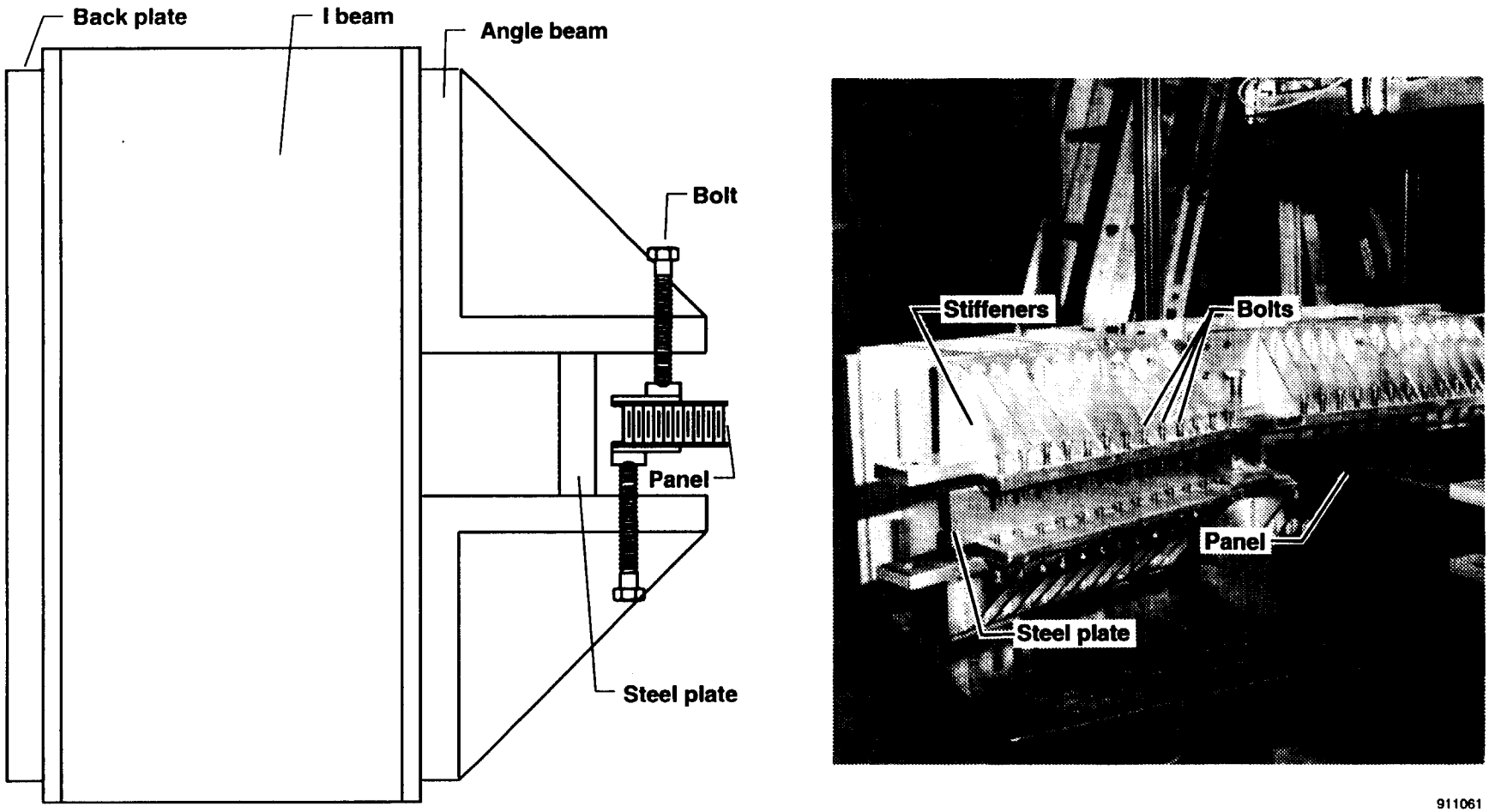

Fig. 9: Final test fixture moment restraint

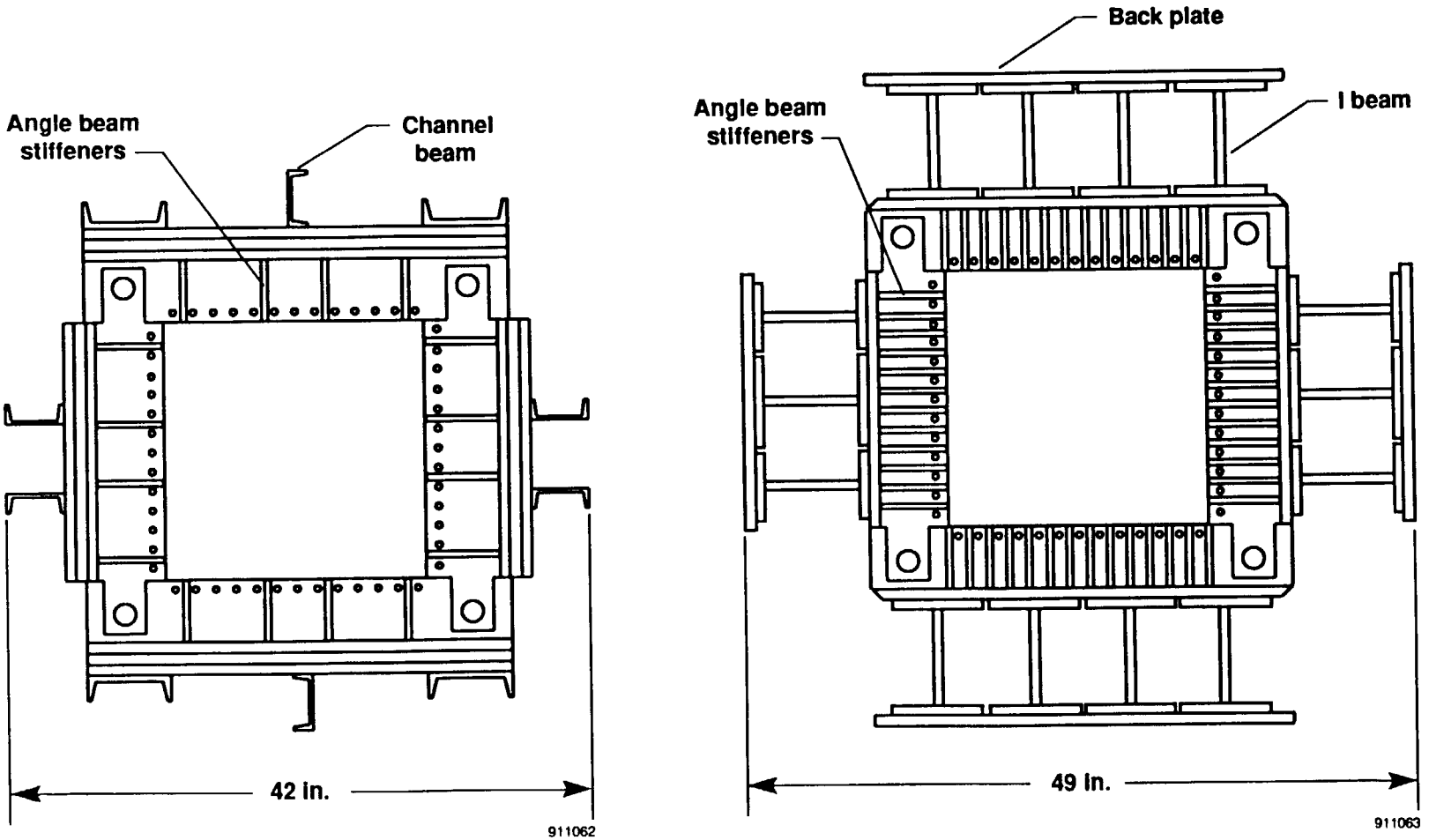

(a) Initial fixture

(b) Final fixture

Fig. 10: Comparison of initial and final test fixtures (top view)

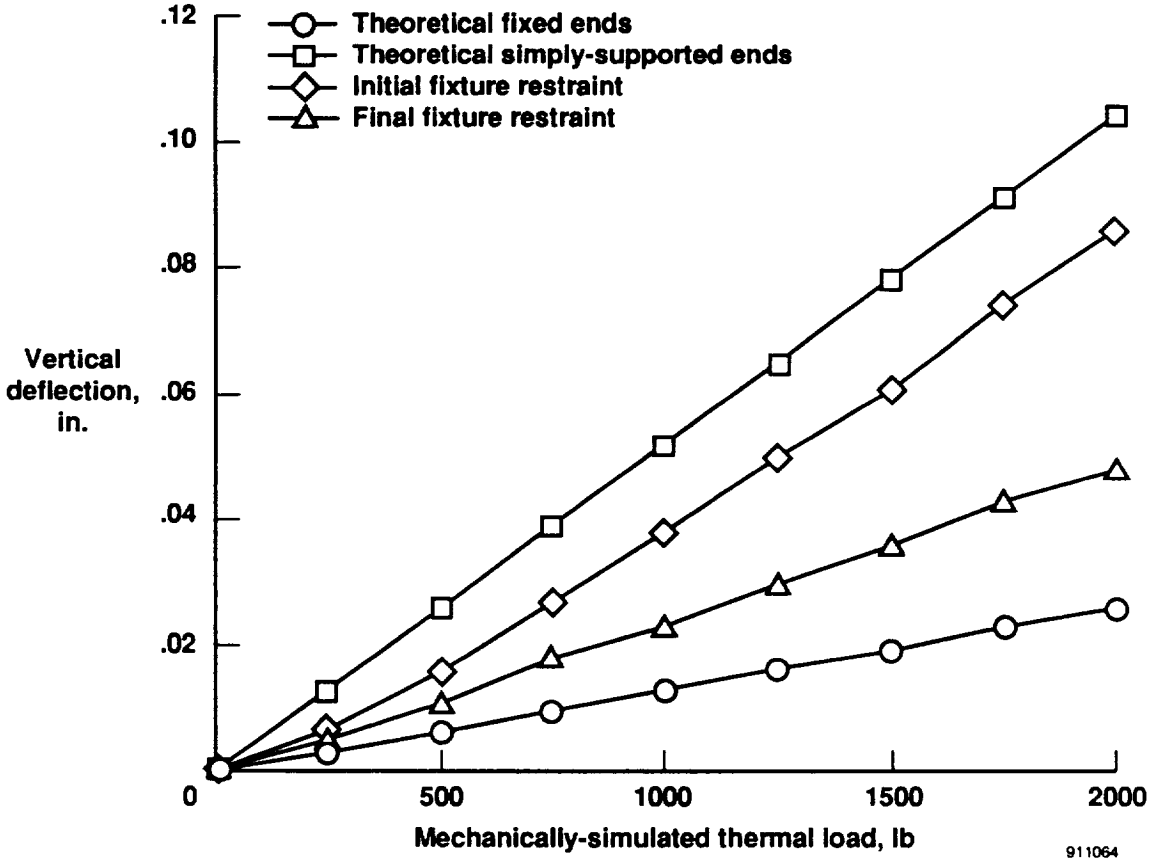

Fig. 11: Edge moment calibration test results

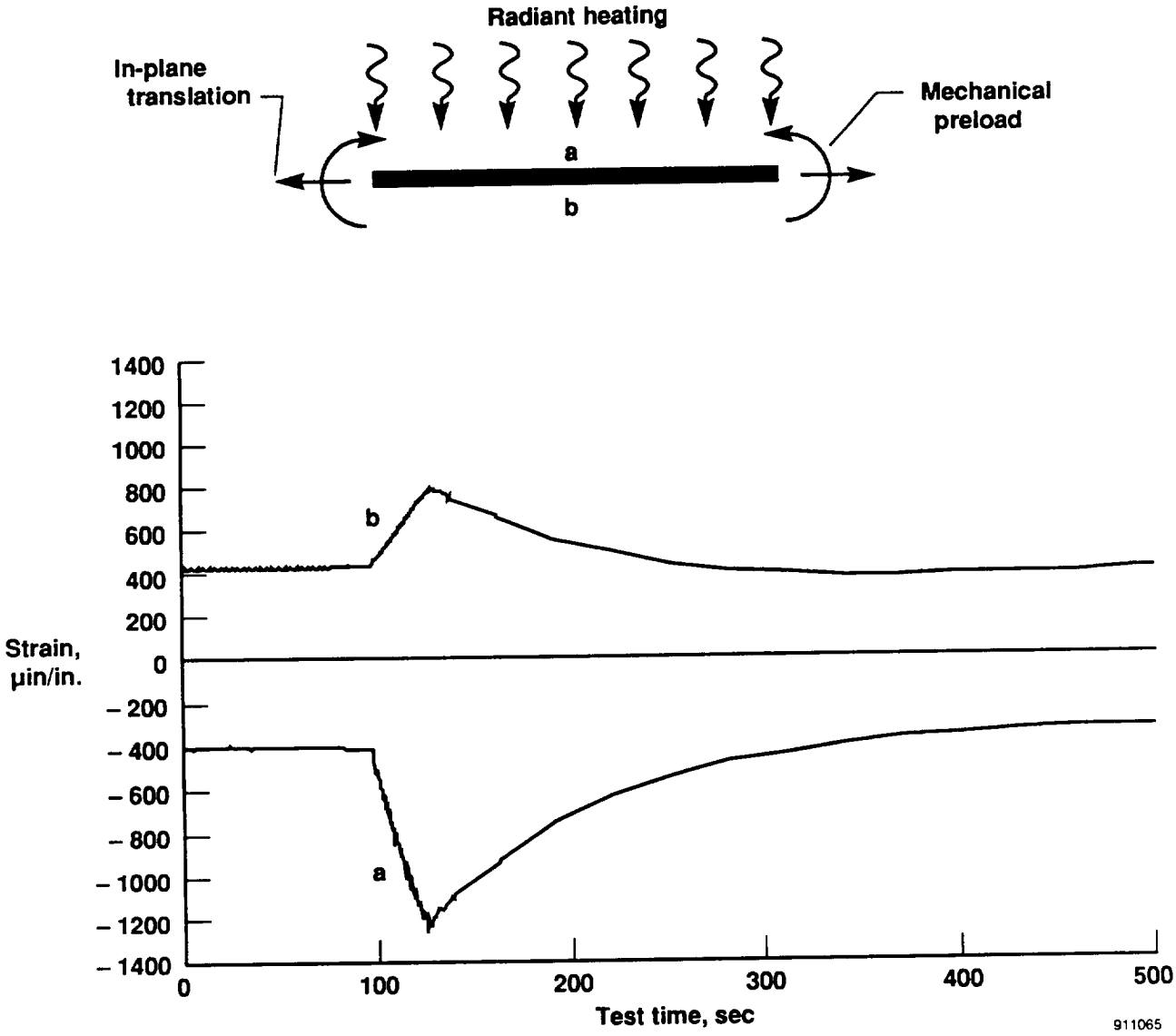

Fig. 12: Time history of strain levels for a 600 °F test with a mechanical preload

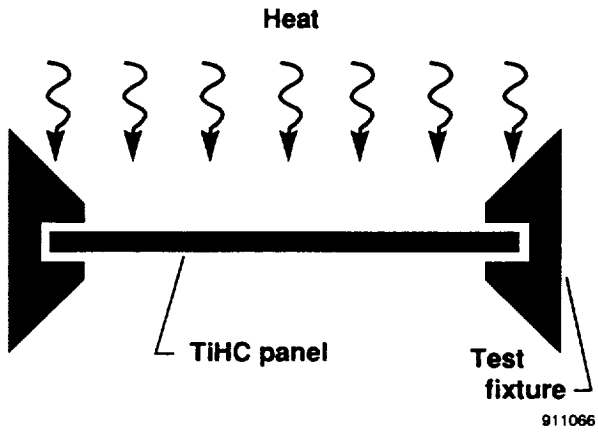

(a) Applied thermal loads

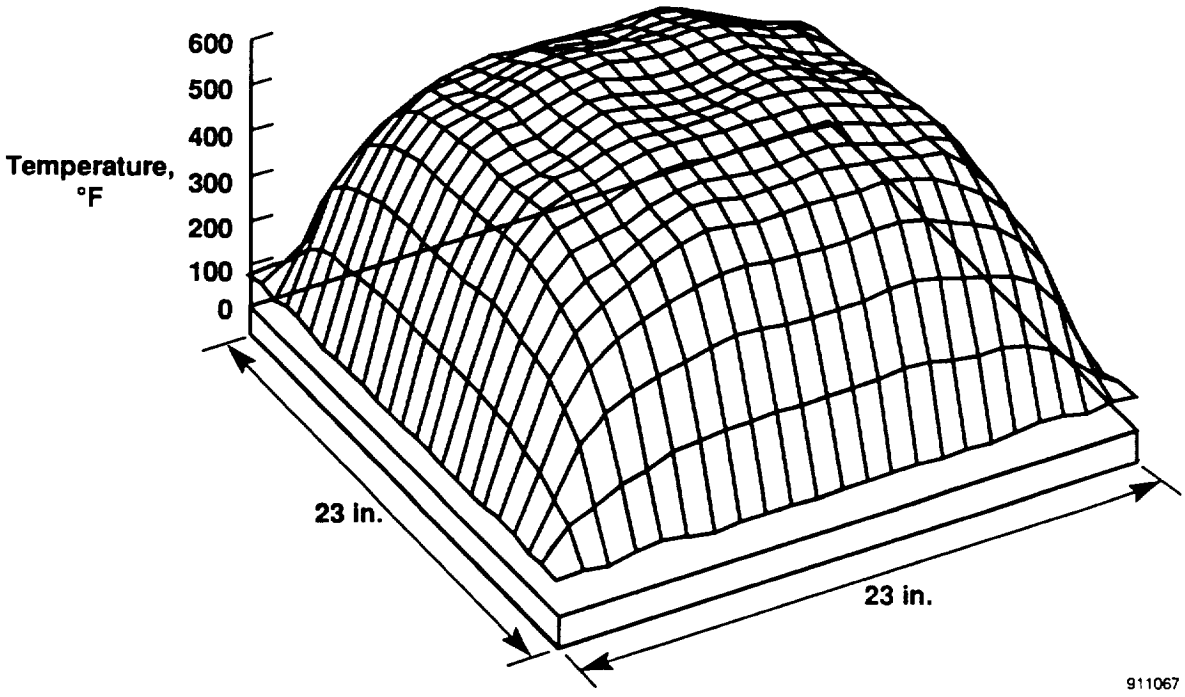

(b) Surface plot of measured temperature distribution

Fig. 13: Temperature distribution resulting from applied thermal loads

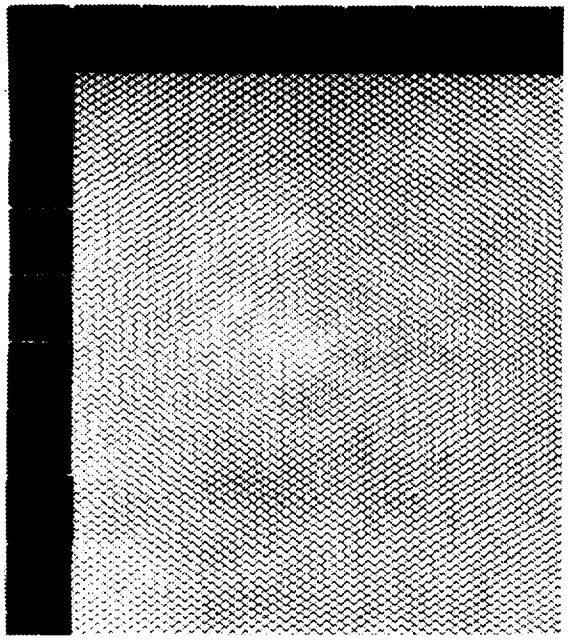

Fig. 14: TiHC panel x ray

REPORT DOCUMENTATION PAGE

Form Approved
OMB No. 0704-0188

1. AGENCY USE ONLY (Leave blank)	2. REPORT DATE	3. REPORT TYPE AND DATES COVERED
	October 1996	Technical Memorandum

4. TITLE AND SUBTITLE

Titanium Honeycomb Panel Testing

5. FUNDING NUMBERS

WU 505-63-40

6. AUTHOR(S)

W. Lance Richards and Randolph C. Thompson

7. PERFORMING ORGANIZATION NAME(S) AND ADDRESS(ES)

NASA Dryden Flight Research Center
P.O. Box 273
Edwards, California 93523-0273

8. PERFORMING ORGANIZATION REPORT NUMBER

H-2133

9. SPONSORING/MONITORING AGENCY NAME(S) AND ADDRESS(ES)

National Aeronautics and Space Administration
Washington, DC 20546-0001

10. SPONSORING/MONITORING AGENCY REPORT NUMBER

NASA TM-4768

11. SUPPLEMENTARY NOTES

Presented at the Structural Testing Technology at High Temperature Conference, Society for Experimental Mechanics, Inc., Dayton, Ohio, Nov. 4–6, 1991. W. Lance Richards, NASA Dryden Flight Research Center, Edwards, California; Randolph C. Thompson, PRC Inc., Edwards, California.

12a. DISTRIBUTION/AVAILABILITY STATEMENT

Unclassified—Unlimited
Subject Category 39

12b. DISTRIBUTION CODE

13. ABSTRACT (Maximum 200 words)

Thermal–mechanical tests were performed on a titanium honeycomb sandwich panel to experimentally validate the hypersonic wing panel concept and compare test data with analysis. Details of the test article, test fixture development, instrumentation, and test results are presented. After extensive testing to 900 °F, non-destructive evaluation of the panel has not detected any significant structural degradation caused by the applied thermal–mechanical loads.

14. SUBJECT TERMS

Elevated temperatures, Hypersonic vehicle, Strain gages, Structural analysis, Structural testing, Test techniques

15. NUMBER OF PAGES

21

16. PRICE CODE

AO3

17. SECURITY CLASSIFICATION OF REPORT	18. SECURITY CLASSIFICATION OF THIS PAGE	19. SECURITY CLASSIFICATION OF ABSTRACT	20. LIMITATION OF ABSTRACT
Unclassified	Unclassified	Unclassified	Unlimited